National Radio Astronomy Observatory Tucson, Arizona

Equipment and Calibration Status for the NRAO 12 Meter Telescope

J. G. Mangum
(jmangum@nrao.edu)

September 21, 1999

Contents

Table 1: 12 Meter Receiver Characteristics

Receiver[a]	Wavelength Range (mm)	Approximate T_{sys}(SSB)[b] (K)
68–90 GHz SIS	4.4–3.3	170–225
90–116 GHz SIS	3.3–2.6	160–350 @ 115 GHz
130–170 GHz SIS	2.3–1.8	180–400
200–265 GHz SIS[c]	1.5–1.1	400–900
260–300 GHz SIS	1.15–1.0	800–1200
215–245 GHz 8-Beam SIS	1.4–1.3	700

[a] All single-beam receivers have two orthogonal polarization channels.
[b] Receiver temperatures include all receiver optics.
[c] Receiver noise is around 200 K single sideband for most of the band, but increases somewhat at the high-frequency end of the band.

1 Introduction

This report summarizes the current status of equipment and system calibration at the NRAO 12m telescope. It is organized into two general sections: one describing the status of the major telescope systems (receivers, backends, subreflector, etc.) and a second which describes the current calibration characteristics of the telescope (efficiencies, beam sizes, etc.). This report will be updated at least once every year and will be available from the NRAO Tucson home page (http://www.tuc.nrao.edu/12meter.html).

2 Telescope Systems

2.1 Receivers

The standard receiver system at the 12m consists of a 4 K closed-cycle cryostat containing up to 8 SIS receivers. A complete set of dual-channel, 600 MHz bandwidth, SIS receivers is operational over the atmospheric windows from 68 to 300 GHz range. Table 1 indicates current performance.

Note that the effective system temperature is defined as

$$T^*_{sys} = \frac{\left(1 + \frac{G_i}{G_s}\right)[T_{rx} + T_A(sky)]}{\eta_l \eta_{fss} \exp(-\tau_0 A)} \tag{1}$$

where

G_i is the image sideband gain;

G_s is the signal sideband gain;

T_{rx} is the receiver DSB noise temperature;

$T_A(sky)$ is the temperature of the sky (definition given below);

η_l is the rear spillover, blockage, scattering, and ohmic efficiency;

η_{fss} is the forward spillover efficiency;

τ_0 is the atmospheric optical depth at 1 airmass (the zenith); and,

A is the number of airmasses, generally given by 1/sin(elevation).

$T_A(sky)$ is given by the equation

$$\begin{aligned} T_A(sky) &= T_{sky} + T_{ant} + T_{cmbr} \\ &= \eta_l T_m \left[1 - \exp(-\tau_0 A)\right] + (1-\eta_l) T_{spill} + \eta_l T_{bg} \exp(-\tau_0 A) \end{aligned} \quad (2)$$

where

T_m is the mean atmospheric temperature,

T_{spill} is the spillover temperature, and

T_{bg} is the cosmic background temperature.

Note that T_m, T_{spill}, and T_{bg} are actually equivalent Rayleigh-Jeans temperatures of the point on the Planck blackbody curve corresponding to the same frequency. This correction factor is given by

$$J(\nu, T) = \frac{h\nu}{\exp\left(\frac{h\nu}{kT}\right) - 1}, \quad (3)$$

where ν is the observing frequency, T is the kinetic temperature, and h and k are the Planck and Boltzmann constants, respectively. For simplicity, we will retain the symbol "T" for temperatures, but in calculations "T" should be replaced by "J(ν,T)".

2.2 Spectrometers

The Observatory maintains two spectrometer systems, filter banks and a correlation spectrometer (the Millimeter Autocorrelator, or MAC). Table 2 lists the filter-bank spectrometers which are available, while Table 3 lists the instrumental parameters for the MAC. Both spectrometers are available for all spectroscopic observing modes, including On-The-Fly (OTF) observing.

For the filter bank spectrometers, the multiplexer will provide two spectra with a total number of spectral channels not in excess of 512. Thus, it is always possible to record simultaneously the output of two filter banks. Except for the 30 kHz bank, all of the filter banks have two independent 128 channel sections. You can configure these banks in one of two ways. In the "series" option, the two sections are placed end to end in frequency space, *i.e.*, the 256 channels are sequential in frequency. In the "parallel" mode, the two sections are used independently to accept different receiver (polarization) channels. The series mode is appropriate for observations requiring a large bandwidth. The parallel mode is useful for narrow band observations in which two different frequency resolutions are needed.

The MAC has a wide variety of spectral resolution modes (see Table 3). Observers can also use the channel windowing option in the correlator setup to select just the channel range they want written to each spectrum. By default, the outer $\frac{1}{8}$ of each spectrum is clipped before being written to the raw data files (the "Usable Channels" listed in Table 3).

Table 2: 12 Meter Filter Spectrometer Characteristics

Filter Resolution[a]	Channels per Bank	Filter Banks Available
2 MHz	256	2
1 MHz	256	2
500 kHz	256	1
250 kHz	256	1
100 kHz	256	1
30 kHz[b]	128	1

[a]**NOTE:** This is the FWHM channel width. See the User's Manual for further details.

[b]Series option only.

2.3 Nutating Subreflector

The nutating subreflector at the 12 Meter is used for beam switched observations in both spectral line and continuum modes. The total beam throw can be varied between 0 and $\pm 4.5'$. For spectral line beam-switched position switching (BSP) measurements, the switch rate can be set to values of 1.25, 2.5, and 5.0 Hz (the default is 1.25 Hz), while for continuum measurements the switch rate is fixed at 4.0 Hz. For BSP measurements, there is no blanking during transitions between ON and OFF measurements due to hardware limitations in the filter banks. Some "accidental" blanking does occur, though, due to the fact that 10 milliseconds of each 100 millisecond dump is spent transfering data. Therefore, the fraction of the total ON source integration time spent on-source is given by Equation 4. Efficiencies as a function of switch throw and rate are shown in Figure 1 for spectral line observations. For beam-switched continuum measurements, the second term in the numerator of Equation 4 is absent. Therefore, as shown in Figure 2, the calibration curve for continuum observations is relatively constant out to about $\pm 3.5'$.

$$\Delta T_{on} = \frac{\left(\frac{0.9}{2f}\right) - (0.125\Delta\theta + 2 - 10)}{\left(\frac{0.9}{2f}\right)} \tag{4}$$

Table 3: Millimeter Autocorrelator (MAC) Configurations

Bandwidth and Channels		Useable Bandwidth and Channels[1]		$\Delta\nu^2$	Resolution
(MHz)	Channels	(MHz)	Channels	(kHz)	(kHz)
2 IF Modes					
800	2048	600*	1536	390.6	781.2
800	4096	600	3072	195.3	390.6
400	4096	300*	3072	97.6	195.3
400	8192	300	6144	48.8	97.6
200	8192	150*	6144	24.4	48.8
200	16384	150	12288	12.2	24.4
100	16384	75*	12288	6.1	12.2
100	32768	75	24576	3.0	6.1
4 IF Modes					
800	1024	600*	768	781.2	1562.0
800	2048	600	1536	390.6	781.2
400	2048	300*	1536	195.3	390.6
400	4096	300	3072	97.6	195.3
200	4096	150*	3072	48.8	97.6
200	8192	150	6144	24.4	48.8
100	8192	75*	6144	12.2	24.4
100	16384	75	12288	6.1	12.2
8 IF Modes					
800	512	600*	384	1562.5	3125.0
800	1024	600	768	781.2	1562.0
400	1024	300*	768	390.6	781.2
400	2048	300	1536	195.3	390.6
200	2048	150*	1536	97.6	195.3
200	4096	150	3072	48.8	97.6
100	4096	75*	3072	24.4	48.8
100	8192	75	6144	12.2	24.4

[1] The useable bandwidth takes account of the 75% efficiency of the analog filters.

[2] **NOTE:** This is the frequency sampling interval, not the FWHM channel width, for a given channel. The FWHM channel width is 2.0 times this value. See the 12 Meter Users Manual for details.

All values in this table refer to each IF.

Modes tagged with a $*$ are produced by dropping the last half of the lags.

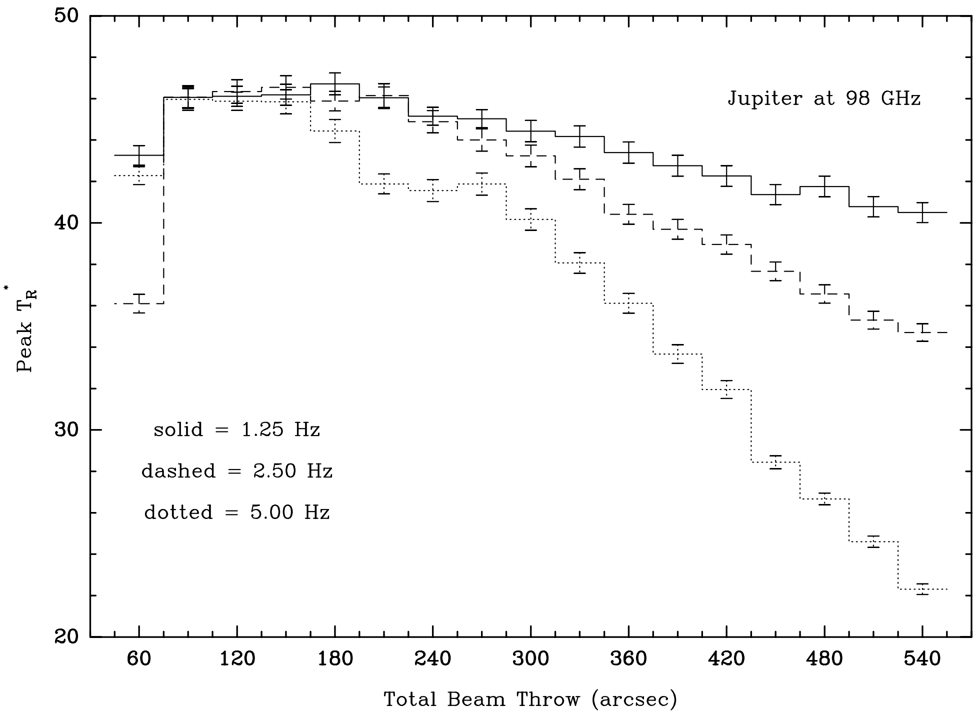

Figure 1: Subreflector efficiency as a function of switch rate and throw for beam switched spectral line observations. For beam throws greater than $\pm 4'$, all three curves fall-off according to Equation 4.

where f is the subreflector switch rate in Hz and $\Delta\theta$ is the total subreflector throw in arcseconds.

3 Calibration Status

This section gives current efficiency and calibration parameters for the 12 Meter Telescope. Table 4 lists a number of standard efficiency parameters, several of which are parameterized in terms of Ruze theory. All efficiency measurements were made at the Cassegrain focus and include the losses of the feed and all optics. Therefore, the Ruze parameters listed include the net effect of the entire telescope and receiving system, not just the primary reflector.

3.1 Beam Alignment

Since all of the 12 Meter receivers are dual polarization, there are two independent beams which must be aligned at the subreflector. This alignment is checked when a receiver is installed. Table 5 lists the measured beam alignment for the 12 Meter receivers. We generally try to adjust the separation between the beams of a receiver to $\leq \frac{1}{10}$th of a beam.

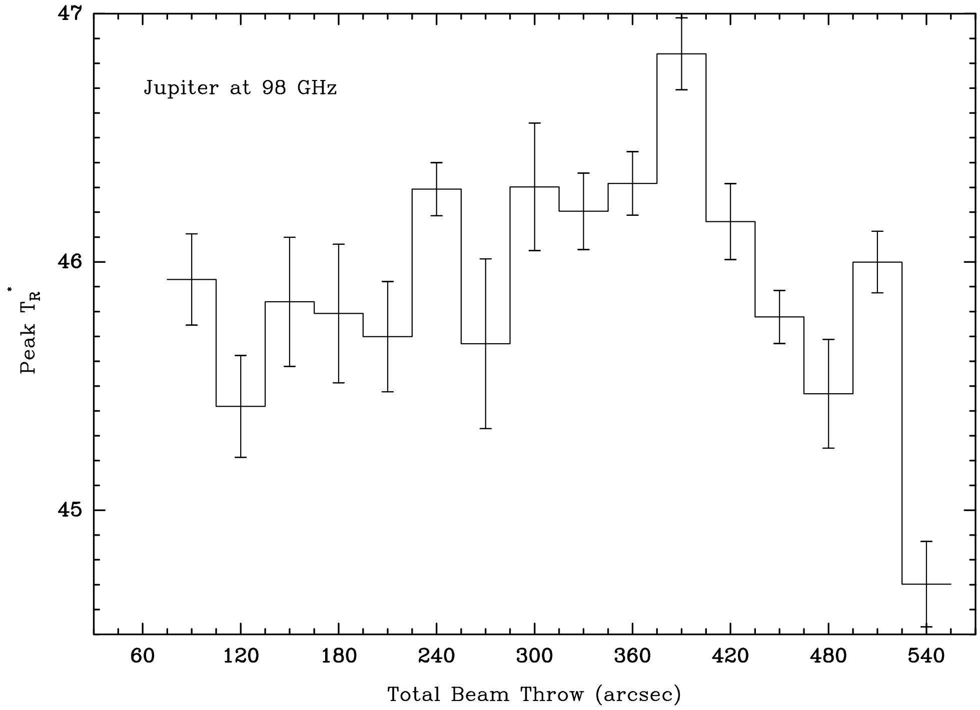

Figure 2: Subreflector efficiency as a function of switch rate and throw for beam switched continuum observations.

Table 4: 12 Meter Telescope Efficiency and Calibration Parameters

Dish Diameter	D	12.0 m
RMS Surface Accuracy	σ	77–85 μm
Infinite Wavelength Aperture Efficiency	η_{A0}	0.52
Surface Deviation Correlation Size	c_σ	28 cm
Feed Taper Factor	κ	1.22
Rear Spillover and Blockage Efficiency	η_l	0.94
Forward Spillover Efficiency	η_{fss}	0.68

Table 5: 12 Meter Telescope Measured Beam Alignment

Receiver	ΔAZ (arcsec)	ΔEL (arcsec)
68–90 GHz SIS	1.9 ± 0.4	2.1 ± 0.3
90–116 GHz SIS	4.3 ± 1.2	0.8 ± 0.7
130–170 GHz SIS	4.9 ± 1.3	2.7 ± 1.5
200–265 GHz SIS	...	...
260–300 GHz SIS	...	...
215–245 GHz 8-Beam SIS	...	...

3.2 Beam Characteristics

Figure 3 shows measurements of the main diffraction beam width as a function of frequency, along with the standard relation

$$\begin{aligned} \theta_M &= \kappa \frac{\lambda}{D} \\ &= \kappa \frac{61836.6}{\nu(GHz)D(m)} \end{aligned} \tag{5}$$

At high frequencies, the azimuth beamwidth is broadened beyond its theoretical width by the astigmatism of the primary reflector.

Figure 4 shows the theoretical extent of the error beam as a function of frequency, given by

$$\theta_E = 2\sqrt{\ln 2}\frac{\lambda}{\pi c_\sigma}, \tag{6}$$

where c_σ is the correlation scale size of surface deviations (see Table 4).

Figure 5 shows the theoretical prediction of the amplitude of the error beam relative to the amplitude of the main beam, given by

$$\frac{A_E}{A_M} = \frac{1}{\eta_{A0}}\left[\frac{2c_\sigma}{D}\right]^2\Big(\exp(\delta^2) - 1\Big), \tag{7}$$

where $\delta = \frac{4\pi\sigma}{\lambda}$ and all of the other parameters in this equation are listed in Table 4.

3.3 Efficiencies

Figure 6 shows the conventional aperture efficiency η_A, conventional main beam efficiency η_M, and the corrected main beam efficiency η_M^* as a function of frequency, defined as follows:

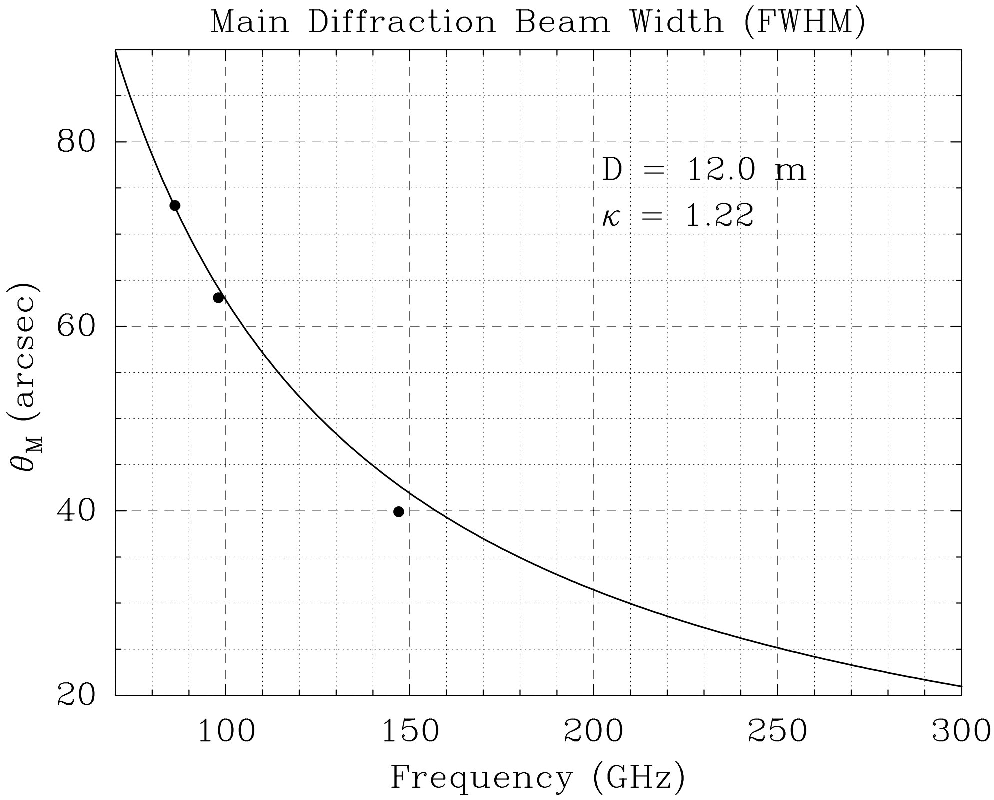

Figure 3: Main diffraction beam width as a function of frequency. Measured values are indicated.

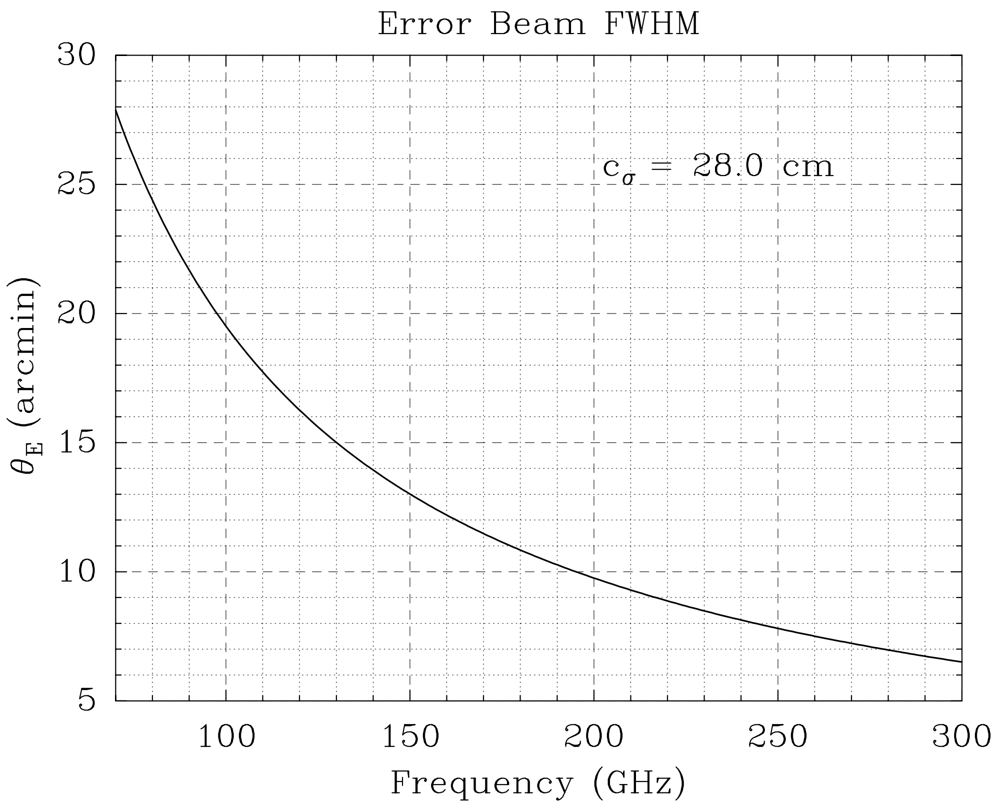

Figure 4: Error beam width as a function of frequency. Since this is only a theoretical estimate, the plotted curve should be used only as a rough estimate of the extent of the error beam.

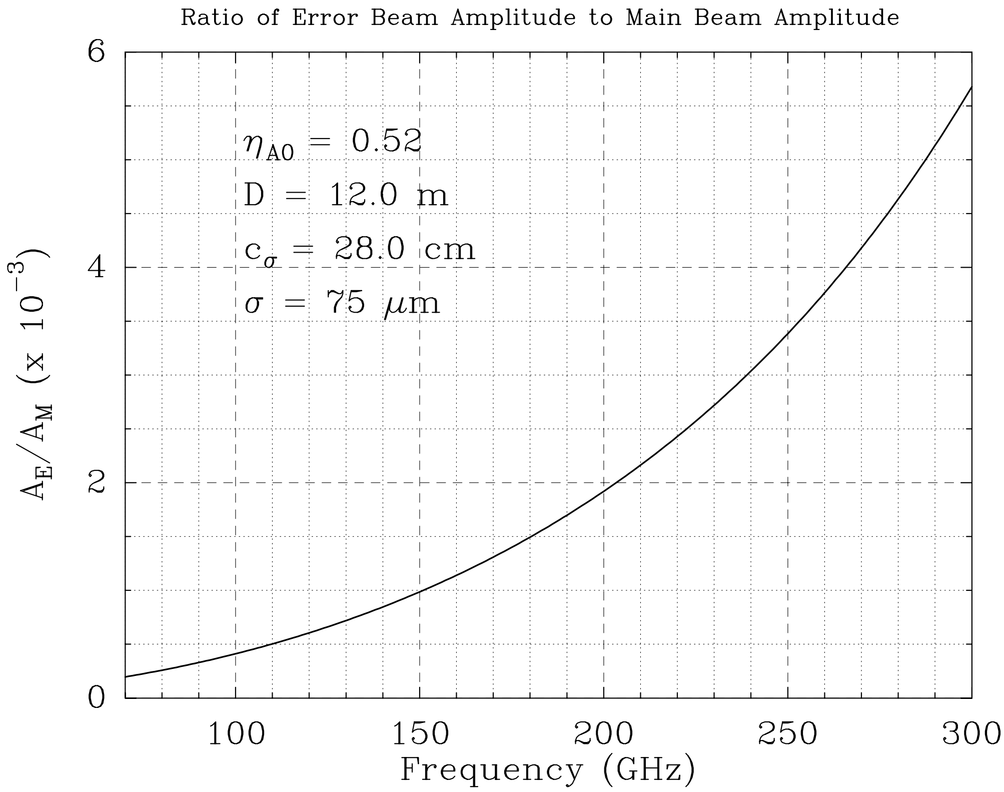

Figure 5: Ratio of error beam amplitude to main diffraction beam amplitude. As with Figure 4, this quantity is based on a theoretical estimate and should be used only as a rough estimate.

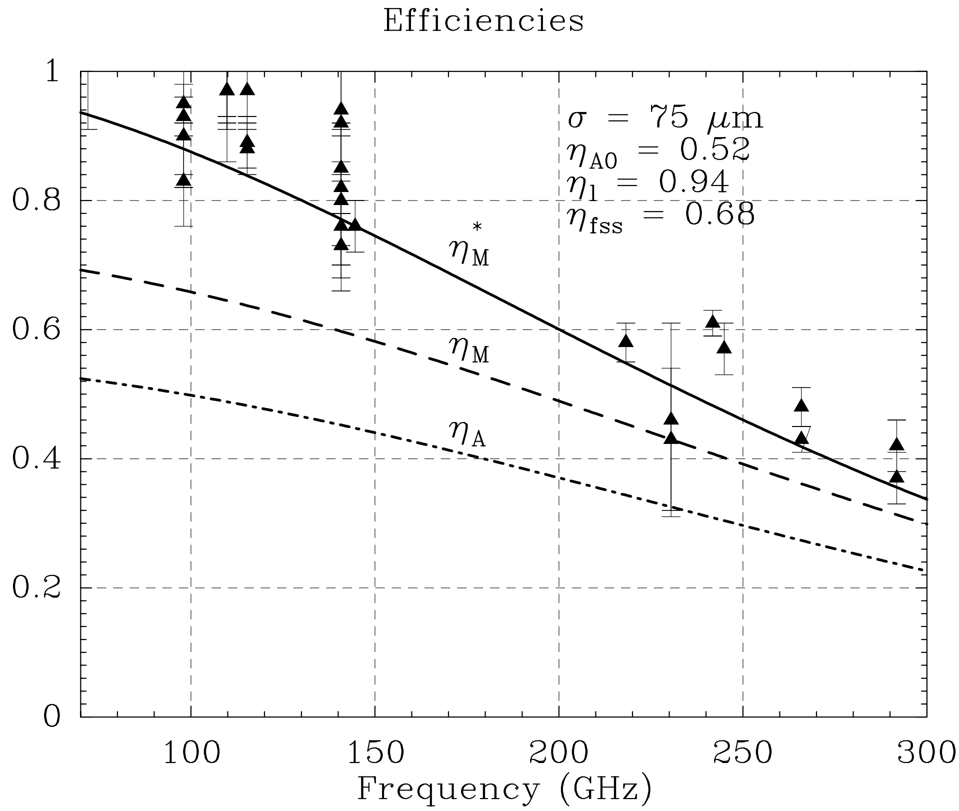

Figure 6: Aperture (η_A), main (η_M), and corrected main (η_M^*) beam efficiencies as a function of frequency. Measured values, which have been obtained over the past year from measurements of the planets, are plotted as solid triangles with associated error bars.

$$\eta_A = \eta_{A0} \exp(-\delta^2) \tag{8}$$

$$\eta_M = \frac{\eta_A A_p \Omega_M}{\lambda^2} \tag{9}$$

$$\eta_M^* = \left[1 + \frac{A_E \theta_E^2}{A_M \theta_M^2}\right] \tag{10}$$

where

$\delta = \frac{4\pi\sigma}{\lambda}$,

$\Omega_M = 1.13\theta_M^2$,

$A_p = 113\ m^2$ (the physical aperture of the 12 Meter),

and the other quantities are given elsewhere in this document. The corrected beam efficiency η_M^* can be used to convert a T_R^* temperature to a main beam brightness temperature, provided that the source is not extended beyond the main beam.

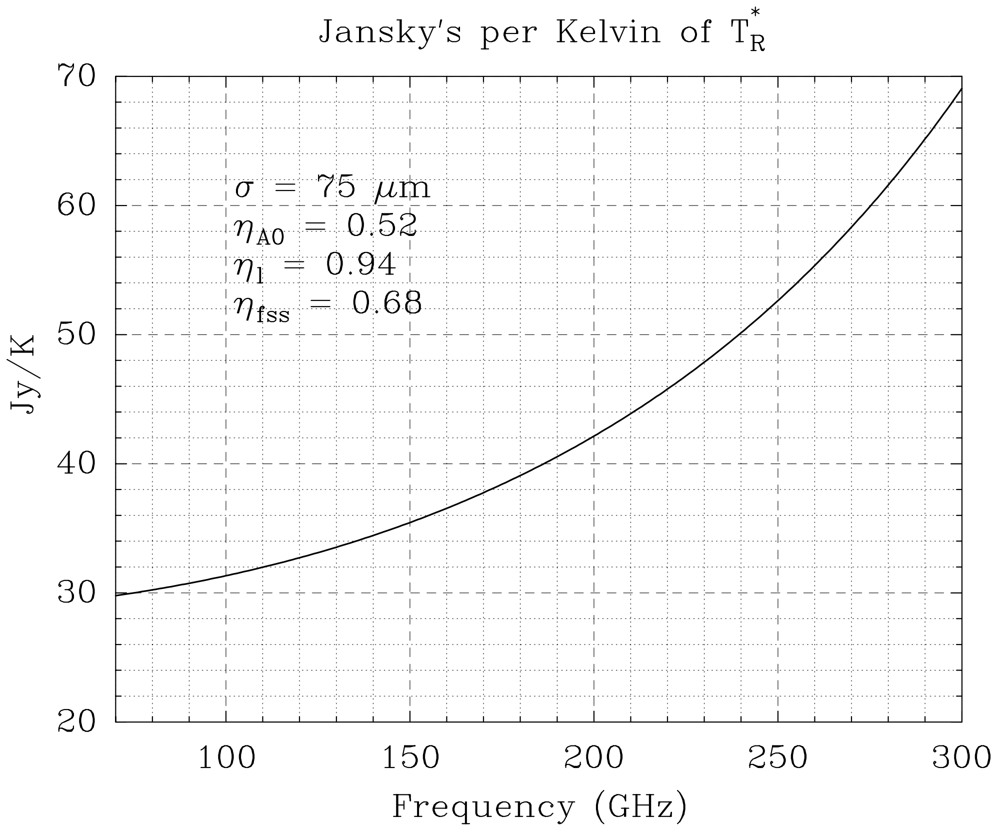

Figure 7: This quantity can be used to convert point source antenna temperatures measured on the vane or chopper wheel calibration scale, T_R^*, to flux densities.

3.4 Jansky's to Kelvin Conversion

To convert point source antenna temperatures, measured on the vane or chopper wheel calibration scale T_R^*, to flux densities, one must use the following relation:

$$\frac{S_\nu}{T_R^*} = \frac{\eta_l \eta_{fss}}{\eta_A} \frac{2k}{A_p} \tag{11}$$

where

k = Boltzmann's constant ($1.380662 \times 10^{-22} JK^{-1}$),

$\frac{2k}{A_p}$ = 24.4155 Jy K^{-1} for the 12 Meter.

A plot of this relation as a function of frequency is shown in Figure 7.